

# Filamentation without intensity clamping

P. Prem Kiran,<sup>1,2</sup> Suman Bagchi,<sup>1,2</sup> Cord L. Arnold,<sup>3</sup>  
Siva Rama Krishnan,<sup>4</sup> G. Ravindra Kumar,<sup>1</sup> and Arnaud Couairon<sup>5</sup>

<sup>1</sup>Tata Institute of Fundamental Research, I, Homi Bhabha Road, Mumbai 400005, India

<sup>2</sup>ACRHEM, University of Hyderabad, Gachibowli, Hyderabad 500046, India

<sup>3</sup>Laboratoire d'Optique Appliquée, École Nationale Supérieure des Techniques Avancées - École Polytechnique, CNRS, F-91761 Palaiseau, France

<sup>4</sup>Department of Physics, Sri Sathya Sai University, Prasanthi Nilayam P.O. 515134, India

<sup>5</sup>Centre de Physique Théorique, École Polytechnique, CNRS, F-91128 Palaiseau, France

[\\*couairon@cpt.polytechnique.fr](mailto:couairon@cpt.polytechnique.fr)

**Abstract:** We present measurements of the supercontinuum emission (SCE) from ultrashort Ti:Saph laser pulse filamentation in air in a tightly focused geometry. The spectral broadening of SCE indicates that peak intensities exceed the clamping value of a few  $10^{13}$  W/cm<sup>2</sup> obtained for filamentation in a loose focusing geometry by at least one order of magnitude. We provide an interpretation for this regime of filamentation without intensity clamping.

© 2010 Optical Society of America

**OCIS codes:** (190.5940) Self-action effects; (190.6135) Spatial solitons; (190.5530) Pulse propagation and temporal solitons.

## References and links

1. A. Dubietis, E. Gaizauskas, G. Tamošauskas, and P. Di Trapani, "Light Filaments without Self-Channelling," *Phys. Rev. Lett.* **92**, 253903 (2004).
2. A. Couairon and A. Mysyrowicz, "Femtosecond filamentation in transparent media," *Phys. Rep.* **441**, 47–189 (2007).
3. F. Belgiorno, S. L. Cacciatori, G. Ortenzi, V. G. Sala, and D. Faccio, "Quantum Radiation from Superluminal Refractive-Index Perturbations," *Phys. Rev. Lett.* **104**, 140403 (2010).
4. C. D'Amico, A. Houard, S. Akturk, Y. Liu, J. Le Bloas, M. Franco, B. Prade, A. Couairon, V. T. Tikhonchuk, and A. Mysyrowicz, "Forward THz radiation emission by femtosecond filamentation in gases: theory and experiment," *N. J. Phys.* **10**, 013015 (2008).
5. S. Suntsov, D. Abdollahpour, D. G. Papazoglou, and S. Tzortzakis, "Efficient third-harmonic generation through tailored IR femtosecond laser pulse filamentation in air," *Opt. Express* **17**, 3190 (2009).
6. S. Suntsov, D. Abdollahpour, D. G. Papazoglou, and S. Tzortzakis, "Filamentation produced third harmonic in air via plasma enhanced third-order susceptibility," *Phys. Rev. A* **81**, 033817 (2010).
7. G. Méchain, A. Couairon, Y.-B. André, C. D'Amico, M. Franco, B. Prade, S. Tzortzakis, A. Mysyrowicz, and R. Sauerbrey, "Long-range self-channelling of infrared laser pulses in air: a new propagation regime without ionization," *Appl. Phys. B* **79**, 379–382 (2004).
8. G. Méchain, C. D'Amico, Y.-B. André, S. Tzortzakis, M. Franco, B. Prade, A. Mysyrowicz, A. Couairon, E. Salmon, and R. Sauerbrey, "Range of plasma filaments created in air by a multi-terawatt femtosecond laser," *Opt. Commun.* **247** 171–180 (2005).
9. C. Ruiz, J. San Román, C. Méndez, V. Díaz, L. Plaja, I. Arias, and L. Roso, "Observation of Spontaneous Self-Channelling of Light in Air below the Collapse Threshold," *Phys. Rev. Lett.* **95**, 053905 (2005).
10. P. P. Kiran, S. Bagchi, S. R. Krishnan, C. L. Arnold, G. R. Kumar, and A. Couairon, "Focal dynamics of multiple filaments: Microscopic Imaging and Reconstruction," *Phys. Rev. A* **82**, 013805 (2010).
11. A. A. Ionin, S. I. Kudryashov, S. V. Makarov, L. V. Seleznev, and D. V. Siniitsyn, "Multiple Filamentation of Intense Femtosecond Laser Pulses in Air," *JETP Lett.* **90**, 423 (2009).

12. O. Varela, A. Zair, J. San Román, B. Alonso, I. J. Sola, C. Prieto, and L. Roso, "Above-millijoule super-continuum generation using polarisation dependent filamentation in atoms and molecules," *Opt. Express* **17**, 3630–3639 (2009).
13. W. Liu, S. Petit, A. Becker, N. Aközbeek, C. M. Bowden, and S. L. Chin, "Intensity clamping of a femtosecond laser pulse in condensed matter," *Opt. Commun.* **202**, 189–197 (2002).
14. A. Couairon, H. S. Chakraborty, and M. B. Gaarde, "From single-cycle self-compressed filaments to isolated attosecond pulses in noble gases," *Phys. Rev. A* **77**, 053814 (2008).
15. M. B. Gaarde and A. Couairon, "Intensity Spikes in Laser Filamentation: Diagnostics and Application," *Phys. Rev. Lett.* **103**, 043901 (2009).
16. H. S. Chakraborty, M. B. Gaarde, and A. Couairon, "Single attosecond pulses from high harmonics driven by self-compressed filaments," *Opt. Lett.* **31**, 3662–3664 (2006).
17. H. Yang, J. Zhang, Q. Zhang, Z. Hao, Y. Li, Z. Zheng, Z. Wang, Q. Dong, X. Lu, Z. Wei, Z. Sheng, J. Yu, and W. Yu, "Polarization-dependent supercontinuum generation from light filaments in air," *Opt. Lett.* **30**, 534–536 (2005).
18. A. Couairon, "Light bullets from femtosecond filamentation," *Eur. J. Phys. D* **27**, 159–167 (2003).
19. F. Théberge, W. Liu, P. Tr. Simard, A. Becker, and S. L. Chin, "Plasma density inside a femtosecond laser filament in air: Strong dependence on external focusing," *Phys. Rev. E* **74**, 036406 (2006).
20. D. G. Papazoglou and S. Tzortzakis, "In-line holography for the characterization of ultrafast laser filamentation in transparent media," *Appl. Phys. Lett.* **93**, 041120 (2008).
21. X. Lu, X. L. Liu, T. T. Xi, X. Liu, and J. Zhang, "Tightly focused femtosecond laser pulse induced breakdown in air," in COFIL 2010, abstracts of the 3rd International Symposium on Filamentation, p. 73.

## 1. Introduction

Ultrashort laser pulse filamentation is now widely known as a propagation regime in the form of a narrow intensity peak surrounded by a large energy reservoir allowing both for continuous reconstruction of the hot core by an energy flux from the periphery [1] and for intense laser matter interaction over long distances compared to the Rayleigh length of the peak [2]. Tuning this interaction would not only benefit to fundamental science as recently proposed from the analogy between filamentation and gravitation [3], but also open the way to applications such as the generation of secondary sources of radiation [4–6]. In this paper, we investigate filamentation in air in a tight focusing geometry and show that the peak intensity exceeds the usual value of  $10^{13}$  W/cm<sup>2</sup> by 2 orders of magnitudes.

We use throughout this work the general definition proposed in Ref. [2] which states that *the terms of filaments and filamentation denote a dynamic structure with an intense core, that is able to propagate over extended distances much larger than the typical diffraction length while keeping a narrow beam size without the help of any external guiding mechanism*. This definition includes various filamentation regimes from filaments without plasma channels in loose focusing geometry [7–9] to small scale filaments obtained with large numerical apertures [10, 11]. Among other remarkable features, filamentation is also associated with supercontinuum emission (SCE) covering the visible spectral region and extending towards the infrared wavelengths. A recent work showed that the energy content of the SCE can be enhanced above the millijoule level, opening the way to post-compression of multi-terawatt laser pulses [12]. In a loose focusing geometry, the highest intensity in a filament is clamped by nonlinear effects including multiphoton absorption and plasma defocusing [13, 14]. A criterion characterizing intensity clamping was proposed by Liu *et al.* from measurements of the supercontinuum spectrum of an intense femtosecond laser pulse propagating in condensed optical media: intensity clamping was shown to limit plasma-enhanced self-phase-modulation, resulting in a constant frequency upshift bounding the supercontinuum spectrum of an ultrashort laser pulse undergoing filamentation when the pulse energy is increased [13].

Recent numerical simulations indicated that third harmonic generation within filamentation permit refocusing processes with intensity spikes exceeding the clamping value by a factor of three [15, 16]. Simulations and experiments in a tightly focused geometry suggested that a new filamentation regime exists for which initial focusing plays the main role in the determination of

the highest intensity during interaction with the gas. Intensities exceeding  $10^{15}$  W/cm<sup>2</sup> were numerically demonstrated for large numerical apertures (NA > 0.1) [10]. In this paper, we present measurements of the supercontinuum spectrum of an intense Ti:Saph laser pulse undergoing filamentation in this novel tight focusing regime. We show that spectral broadening does not fulfil the Liu *et al.* criterion and we model the suppression of intensity clamping when NA is increased.

## 2. Measurements of Supercontinuum Emission in air

In the experiment, collimated 800 nm, 45 fs pulses from a Ti:Sapphire laser (Thales Laser, Alpha 10, operated at 10 Hz repetition rate) were tightly focused in air using an off-axis parabolic mirror with a focal length of 16 cm. The input beam diameter was  $30 \pm 1$  mm ( $1/e^2$ ) before the focusing element, leading to an  $f/6$  focusing geometry. The alignment of the parabola was carefully checked both at low intensity from the focal spot size of  $12 \pm 2$   $\mu$ m and at high pulse energy from the circular symmetry of supercontinuum emission. Longitudinal high-resolution images of complete filaments formed by individual pulses in a single frame were monitored in the focal region of highly converging focusing elements as in Ref. [10]. These images showed competition between small scale filaments of various diameter and intensities, extending radially over a 200  $\mu$ m FWHM diameter spot. After the interaction region, SCE was collected by a silica lens and monitored by a CCD coupled spectrometer (S2000, Ocean Optics). A set of calibrated neutral density filters were placed in front of the spectrometer to avoid saturation. SCE spectra were collected for 256 shots to reduce the noise from pulse to pulse fluctuations. The energy input laser pulse energy was measured by means of a powermeter (Gentec). The experiments were done for linear (LP) and circularly polarized (CP) pulses.

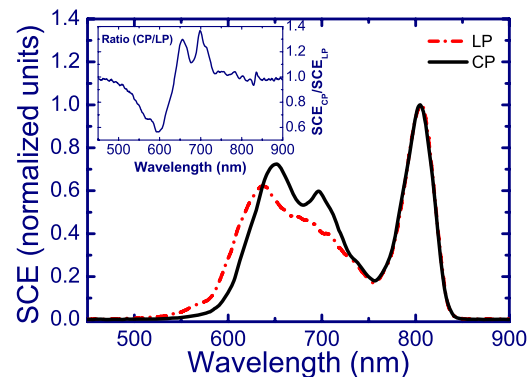


Fig. 1. Typical supercontinuum emission spectrum from the propagation of a linearly polarized (LP) and a circularly polarized (CP) 45 fs laser pulses in air at an input power of  $\sim 100$  GW focused by using  $f/6$  focusing geometry. The inset shows the ratio between the spectral intensities of the CP and LP pulses.

Figure 1 shows typical SCE spectra for LP and CP pulses tightly focused in air for an input power of 100 GW. SCE spectra exhibit a blueshift from the fundamental wavelength that increased with increasing input power. The spectral intensity of SCE observed with CP pulses is smaller than that with LP pulses in the range 400-600 nm and larger in the range 600-750 nm. This observation is consistent with the fact that LP pulses induce ionization of air at a

higher rate than CP pulses with the same energy, which in turn leads to higher plasma enhanced self-phase modulation and a stronger blueshift [17].

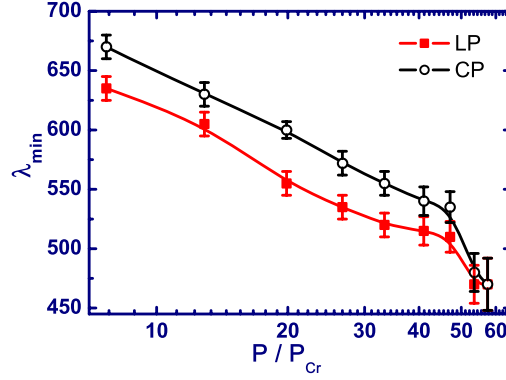


Fig. 2. Minimum wavelength of the supercontinuum emission collected with an off-axis parabola in  $f/6$  focusing geometry for LP and CP pulses.

Figure 2 shows the power dependence of the minimum cutoff wavelength  $\lambda_{\min}$  of the SCE for LP and CP pulses. The minimum wavelength decreases monotonically when the pulse power increases for both polarization states. Therefore, according to the criterion proposed by Liu *et al.* [13] which links intensity clamping to a constant cutoff of SCE, we conclude that no intensity clamping was observed up to input powers of  $60 P_{\text{cr}}$  with a  $f/6$  focusing geometry, where the critical power for self-focusing  $P_{\text{cr}} = 3 \text{ GW}$  denotes a reference value calculated with the nonlinear index coefficient  $n_2 = 3.2 \times 10^{-19} \text{ cm}^2/\text{W}$  [2]. We estimated a lower bound for the peak intensities from the  $200 \mu\text{m}$  width of the energy reservoir. The intensity corresponding to  $50 P_{\text{cr}}$  is  $2.5 \times 10^{14} \text{ W/cm}^2$ , while the standard clamping value in air is a few  $10^{13} \text{ W/cm}^2$  [2]. Small scale filamentation was observed around the focal plane, indicating the presence of even larger peak intensities than those inferred from the homogeneous  $200 \mu\text{m}$  beam. This means that the peak intensity for a small scale filament in a tight focusing configuration largely exceeds the clamping value.

### 3. Modeling of filamentation at high numerical apertures

In order to clarify the scenario of filamentation without intensity clamping, we consider the nucleation of a single small scale filament from the  $200 \mu\text{m}$  large energy reservoir and neglect the interaction between filaments. Following Refs. [2, 18], the filament is described by beam characteristics, i.e. by the filament width  $w(z)$ , power  $P(z)$ , and peak intensity  $I(z) \equiv 2P(z)/\pi w^2(z)$ , the evolution of which is governed by:

$$\frac{dP}{dz} = -\frac{\beta_K}{K} P I^{K-1} \quad (1)$$

$$\frac{d^2 w}{dz^2} = \frac{4}{k_0^2 w^3} \left(1 - \frac{P}{P_{\text{cr}}}\right) + \gamma_{\text{MPI}} \frac{I^K}{w} - \gamma_{\text{MPA}} I^{K-1} \left[ (2K-1) \gamma_{\text{MPA}} w I^{K-1} - 2(K-2) \frac{dw}{dz} \right] \quad (2)$$

Equation (1) describes the power losses due to multiphoton absorption (MPA) with coefficient  $\beta_K = 10^{-94} \text{ cm}^{13} \text{ W}^{-7}$  and  $K = 8$  denotes the number of photons involved in multiphoton ionization (MPI). For simplicity, the model for MPA and MPI considers air as a single species

gas. A comparison with a two species model (oxygen and nitrogen) showed that this approximation is good even when full ionization occurs [10]. Equation (2) describes the evolution of the beam width and accounts for diffraction, Kerr self-focusing with critical power  $P_{\text{cr}}$ , plasma defocusing with coefficient  $\gamma_{\text{MPI}}$  and energy losses. Here  $\gamma_{\text{MPI}} \equiv 2\beta_K T_p \sigma \tau_c / (K+1)^2 \hbar k_0$  where  $\sigma = 8 \times 10^{-20} \text{ cm}^2$  denotes the cross sections for inverse Bremsstrahlung,  $\tau_c = 350 \text{ fs}$  the collision time,  $T_p = 45 \text{ fs}$  the pulse duration and  $\gamma_{\text{MPA}} = [(K-1)\beta_K/2K^2]$ .

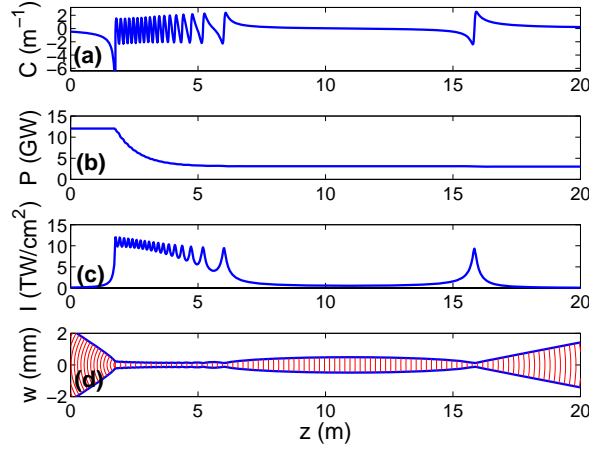


Fig. 3. Typical beam characteristics for filamentation in a loosely focusing regime ( $f = 200 \text{ cm}$ ). (a) beam curvature  $C = w^{-1}dw/dz$ ; (b) power (c) peak intensity and (d) beam width and phase fronts vs propagation distance  $z$ . Input parameters:  $P(z=0) = 4P_{\text{cr}}$ ,  $w(z=0) = 2.25 \text{ mm}$ ,  $f = 2 \text{ m}$ .

Compared to the original system of equations derived in [2,18], Eqs. (1) and (2) are simplified since only the pulse time slice with maximum intensity is considered, while still including the essential ingredients for explaining the absence of intensity clamping. The coefficients of nonlinear effects ( $P_{\text{cr}}^{-1} \propto n_2$ ,  $\beta_K$ ) proportional to the density of non-ionized atoms in the medium, i.e., all physical effects described by Eqs. (1) and (2) except diffraction are switched off when the peak intensity exceeds the intensity threshold  $I_{\text{th}} \equiv (\sigma_K T_p)^{-1/K} \simeq 4 \times 10^{13} \text{ W/cm}^2$  corresponding to full ionization of air with rate  $\sigma_K = 3 \times 10^{-96} \text{ s}^{-1} \text{ cm}^{16} \text{ W}^{-8}$ . Equations (1) and (2) were integrated by a standard Runge Kutta solver for ordinary differential equations with adaptive steps.

#### 4. Numerical results

Figure 3 shows the beam characteristics for a typical filament obtained in loose focusing geometry. In the initial stage ( $z < 2 \text{ m}$ ), self-focusing enhanced by lens focusing dominates. A competition between self-focusing, multiphoton absorption and plasma defocusing then takes place as indicated by the oscillations of the beam curvature  $C = w^{-1}dw/dz$  [Fig. 3(a)], peak intensity [Fig. 3(c)] and filament width [Fig. 3(d)] over  $\sim 15 \text{ m}$  (tens of Rayleigh lengths  $z_0 = 15.7 \text{ cm}$  calculated for a  $200 \mu\text{m}$  width) while the power monotonically decreases due to air ionization [Fig. 3(b)]. In the final stage ( $z > 16 \text{ m}$ ), the beam diffracts. During the filamentation stage ( $2 < z < 16 \text{ m}$ ), the curvature induced by self-focusing never exceeds  $2 \text{ m}^{-1}$  and can be easily compensated by that induced by plasma defocusing. The maximum plasma density (not shown) always corresponds to a weakly ionized gas. The peak intensity remains below a clamping value which does not exceed a few  $10^{13} \text{ W/cm}^2$  in agreement with numerous simulations

and observations [2] and with the criterion of a constant lower bound of the supercontinuum spectrum [13].

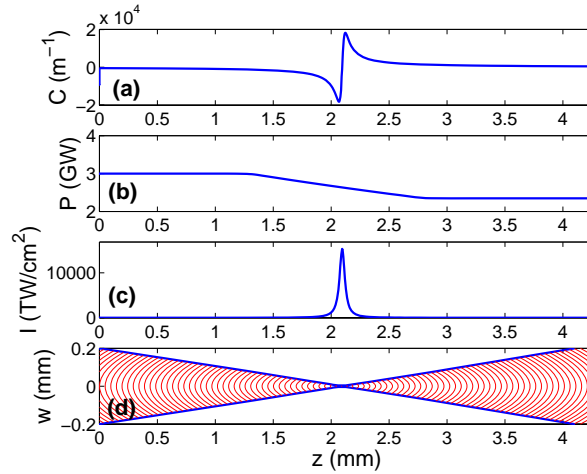


Fig. 4. Same as in Fig. 3 but for a tight focusing geometry. The parameters of the input beam at  $z = 0$  are  $w_0 = 200 \mu\text{m}$ ,  $f = 0.21 \text{ cm}$  (same numerical aperture as in the experiment),  $P = P_{\text{cr}}$  and  $I_0 = 5 \times 10^{12} \text{ W/cm}^2$ .

The results are significantly different for a tight focusing geometry. Figure 4 shows the beam characteristics for a numerical aperture of about 0.11, as in the experiment, over  $\sim 4 \text{ mm}$  around the focus. Due to initial focusing, air becomes fully ionized  $600 \mu\text{m}$  before the focus and the beam curvature is still much larger than that induced by plasma defocusing, as indicated by a comparison of the curvatures in Figs. 4(a) and 3(a) which shows a maximum ratio of  $10^4$ . In tight focusing geometry, the competition between plasma defocusing and self-focusing no longer plays a significant role in intensity clamping. The leading part of the pulse is sufficiently intense to singly ionize all oxygen and nitrogen molecules. The intense part of the pulse then sees a fully ionized plasma channel with quasi flat radial profile, making plasma defocusing inefficient. Plasma absorption remains significant. The intensity exceeds  $10^{15} \text{ W/cm}^2$  over  $\sim 1.2 \text{ mm}$ , i.e. more than 8 Rayleigh lengths. Consequently, a filamentation regime without intensity clamping, close to a breakdown regime, is easily reached with large numerical apertures.

## 5. Conclusion

In conclusion, we have shown that for tight focusing geometries, ultrashort laser pulse filamentation in air does not lead to the standard intensity clamping regime or to a constant minimal cutoff wavelength for the SCE. Previous works demonstrated that external focusing strongly influences the plasma density and the diameter of femtosecond filaments in air and provided measurements of the plasma density up to  $2 \times 10^{19} \text{ cm}^{-3}$  (ionization degree of 0.8) for a numerical aperture of  $\text{NA}=0.11$  [11, 19–21]. Our experiments showed that associating higher pulse energies and a tight focusing geometry leads to a new regime where air is fully ionized and small scale filaments at peak intensity above the clamping value are obtained. We provided a model for the nucleation of a single filament from the energy reservoir valid for small as well as large NA where the main features of filamentation without intensity clamping are reproduced. The model shows that the very high initial curvature of the beam leads to full ionization of the medium, which in turn prevents plasma defocusing to play a significant role in intensity clamping. Although much shorter than in a loose focusing geometry, small scale filamentation

was observed over tens of Rayleigh lengths corresponding to the beam waist [10].

### **Acknowledgements**

GRK acknowledges a DAE-SRC-ORI grant (Government of India).